Master's Thesis of Engineering

Low Work Function Stretchable Polymeric Electrode for Intrinsically Stretchable Organic Light-Emitting Diodes

고유 신축성 발광소자 제작을 위한 낮은 일함수의
고유 신축성 고분자 전극

February 2023

Graduate School of Engineering
Seoul National University
Department of Materials Science and Engineering Major

Hyeokjun Kwon

Low Work Function Stretchable Polymeric Electrode for Intrinsically Stretchable Organic Light-Emitting Diodes

Tae-Woo Lee

Submitting a master's thesis of Public Administration

February 2023

Graduate School of Engineering
Seoul National University
Department of Materials Science and Engineering

Hyeokjun Kwon

Confirming the master's thesis written by
Hyeokjun Kwon
Month Year

Chair	Jeong-Yun Sun	(Seal)
Vice Chair	Tae-Woo Lee	(Seal)
Examiner	Min Sang Kwon	(Seal)

Abstract

Keyword : PEDOT:PSS, Intrinsically stretchable electrode, Polyethyleneimine, De-doping of PEDOT:PSS
Student Number : 2021-20859

The poly (3,4-ethylenedioxythiophene):poly(styrene sulfonate) (PEDOT:PSS) is a promising candidate for intrinsically stretchable electrodes to replace brittle and high-cost ITO. Previously, the study on stretchable PEDOT:PSS was only focused on electrical conductivity and mechanical stretchability. However, to be used as electrode in intrinsically stretchable light-emitting diode (ISOLED), energy level alingment is importnat for better charge injection. The work function (WF) of pristine PEDOT:PSS is around 5 eV. Therefore, the WF lowering must be conducted to use PEDOT:PSS as cathode in ISOLED. We use polyethyleneimine (PEI) which is widely used WF modifying layer to lower the WF of stretchable PEDOT:PSS. Commonly when PEI is directly coated on PEDOT:PSS, an undesired chemical reaction occurs where the PEI and PEDOT:PSS interacts. This reaction is called de-doping of PEDOT:PSS and the electrcial conductivity is significantly decreased. Especially in stretchable PEDOT:PSS with large fibril structure, PEI can diffuse into PEDOT:PSS film, therefore there are more de-doping of PEDOT:PSS. . Here, we introduce a PEDOT:PSS surface modification to tune the microstructure of stretchable PEDOT:PSS. The achieved smaller fibril structure effectively prevent the diffusion of PEI and chemical reaction can be suppressed only at the surface. Finally, we can achieve a PEDOT:PSS cathode with low WF (3.84 eV) without sacrificing any electrical conductivity. We succesfully fabricate ISOLED by based on low WF stretchable PEDOT:PSS.

Table of Contents

List of Figures

List of Tables

Chapter 1. Introduction

The next generation display will be on the skin with the increasing demand for wearable electronics, therefore display should be stretchable like human skin. The intrinsically stretchable display is consist of stretchable materials such as polymer[1-2] and nanomaterial[3-5] which can show superior ductilities compare to its counterpart that uses specific geometrical patterning[6-11].

To achieve an intrinsically stretchable display, every interlayer needs to be stretchable. Especially, achieving the stretchable electrode is highly challenging because there is a tradeoff between mechanical ductilities and electrical conductivities. Poly (3,4-ethylene dioxythiophene): poly (styrene sulfonic acid) (PEDOT: PSS) is a promising candidate for intrinsically stretchable electrode because this conducting polymer can achieve both stretchability and electrical conductivity.[12] The pristine PEDOT: PSS shows low conductivity (< 1S/cm), and low stretchability. The poor electrode characteristics can be enhanced dramatically by various types of additives. With a little amount of polar solvents such as DMSO[13-14], or ethylene glycol[15], the conductivity of PEDOT: PSS can be increased over 500 S/cm. A surfactant such as Triton X-100[16-17] or Zonyl[18-19] can enhance the stretchability of PEDOT:PSS. Lastly, Ionic liquids have been reported that it can increase both conductivity and stretchability.[12, 20-21] However, previous works are only focused on enhancing conductivity or stretchability, so stretchable

PEDOT:PSS is usually demonstrated as interconnects or anodes for hole injection[22].

The WF of PEDOT:PSS is known to be around 5.0 eV, therefore to be used as a cathode for electron injection in a light-emitting diode (LED), WF lowering must be achieved. Polyethyleneimine (PEI) is a non-conjugated polymer, rich in amine groups which can effectively decrease the WF of the film when it is overcoated.[23] This material can create strong interfacial dipoles on the surface of the films to decrease the WF. When PEI is directly coated onto the PEDOT:PSS, there are two possible reactions that can occur at the interface.[24-26] Firstly, coulombic interaction between PSS^- and NR_m^+ from PEI. The other one is that aliphatic amines can lead to a series of proton and electron transfer reactions that can lead to neutral PEDOT. This neutral state of PEDOT is highly undesired for electronics, especially where PEDOT: PSS is used for the electrode. Because this neutral state lacks polaron or bipolaron.[27-28] This transition from doped PEDOT to neutral PEDOT is called de-doping of PEDOT:PSS. To use PEDOT:PSS as an electron injection electrode, therefore this trade-off between WF lowering and decrease of electrical conductivity must be solved.

In this work, we found there is severe de-doping of PEDOT in stretchable PEDOT:PSS film that has a fibril structure. The microstructure of stretchable PEDOT:PSS is known to be a fibril structure with expanded volume.[18] When PEI

is overcoated onto fibril structure of stretchable PEDOT:PSS, the diffusion of PEI into stretchable PEDOT:PSS film is much easier, leading more de-doping of PEDOT.[29] As a results, there are significant decrease of electrical conductivity in stretchable PEDOT:PSS after PEI coating. Therefore, to achieve highly conductive stretchable PEDOT:PSS with low WF, it is key to prevent the diffusion of PEI into PEDOT:PSS film. We introduced selective etching post treatment (SEPT) with the different polarity of the solvent, to tune the microstructure of stretchable PEDOT:PSS. With SEPT, the microstructure of stretchable PEDOT:PSS has changed from larger fibril into smaller fibril, and the diffusion of PEI into PEDOT:PSS film can be successfully prevented. This means that the PEI interacted region is only limited at the interface, so the PEDOT that can be de-doped by PEI is also limited to PEDOT that is located at the interface. With this SEPT process before spin coating PEI, we could achieve highly conductive, stretchable and transparent polymeric electrodes with low WF. Our stretchable polymeric electrode shows a work function of around 3.82 eV with a sheet resistance of 232 ohm/sq which is adequate to be used as an electron injection electrode for stretchable light-emitting diodes.

Chapter 2. Results and Discussions

2.1 Fabrication of Low Work Function Stretchable PEDOT:PSS

To obtain a stretchable and conductive PEDOT:PSS electrode, certain amount of dimethyl sulfoxide (DMSO) and Triton X-100 (Tx) was added into the PEDOT:PSS solution. These additives are known to increase the conductivity and stretchability of PEDOT:PSS by inducing phase separation between PEDOT and PSS by charge scattering effect.[5] The PEDOT:PSS solution is then coated on Styrene Ethylene/Butylene Styrene (SEBS) which is a stretchable elastomer substrate. The PEI is then overcoated onto PEDOT:PSS to lower the WF of stretchable PEDOT:PSS film. When thin PEI film is formed onto PEDOT:PSS film, then interfacial dipole is formed at the surface of PEI. This interfacial dipole from amine groups of PEI can effectively lower the work function, which is sufficient to be used as a PEDOT:PSS cathode for electron injection. Figure 1 illustrates the process for fabricating a low WF stretchable PEDOT:PSS electrode including additional post treatment in this research.

2.2 De-doping of PEDOT:PSS with PEI

When PEI interacts with PEDOT:PSS, however, there is an undesired reaction between PEDOT and PEI at the interface. The amine groups of PEI change into protonated amine groups which leads to the molecular dipole in PEI. This molecular dipole at the surface can role as an interfacial dipole which was mentioned in at earlier chapter. However, when the molecular dipole is nearby PEDOT:PSS, the undesired reaction between PEDOT:PSS and PEI are favorable. The undesired reaction is a chemical reaction that is called as 'de-doping of PEDOT. This is that positively charged doped PEDOT then becomes neutral PEDOT with donated electrons from PEI molecular dipole(Figure 2).[26] It was previously reported that the tertiary amine groups are more easily de-dope PEDOT:PSS compare to secondary and primary amine groups. Therefore, we expect that donated electron from PEI is mostly from tertiary group at the PEI carbon backbone, not primary groups.

De-doping of stretchable PEDOT:PSS with PEI was identified by UV absorbance and optical color change. Fabiano's group reported that neutral PEDOT shows UV absorbance peak around 600 nm, and has the optical color of dark blue.[24] In figure 3 (a), (b), the stretchable PEDOT:PSS shows characteristics of neutral PEDOT when PEI is over-coated. Therefore, it is confirmed that this undesired reaction between PEDOT and PEI is the origin of electrical conductivity

sacrifice while lowering the work function of stretchable PEDOT:PSS (Figure 3 (c)).

We found that de-doping of PEDOT is severe in stretchable PEDOT:PSS compare to PEDOT:PSS without additives (Table 1). It is widely reported that the microstructure of stretchable PEDOT:PSS is a fibril structure.[18] By AFM phase image, the fibril structure is confirmed with the addition of Tx 5 wt% which is an experimental condition of our stretchable film (Figure 4 (b)). We assume that severe de-doping in stretchable PEDOT:PSS is because of the fibril structure of PEDOT:PSS. Figure 5 is a schematic illustration that shows the easier PEI diffusion at the stretchable PEDOT:PSS. Without surfactant treatment, the microstructure of PEDOT:PSS has a smaller fibril structure (Figure 5(a)). In this film, PEI exists only at the interface after over-coated, meaning that PEDOT only at the interface can be de-doped by PEI. Large fibril structure with the expanded volume of stretchable PEDOT:PSS, however, makes PEI diffuse easier into PEDOT:PSS film. More PEDOT can be de-doped with the severe PEI diffusion into PEDOT:PSS film (Figure 5(b)).

2.3 The Mechanism of Selective Etching Post Treatment

We found that simple spin coating process with organic solvents can tune the microstructure of PEDOT:PSS. The selective etching post treatment (SEPT) can tune the microstructure of stretchable PEDOT:PSS from large fibril to smaller fibril.

The underlying mechanism of SEPT is removing excess polymers and molecules at the surface of stretchable PEDOT:PSS. D. Kang's group. reported that PEDOT:PSS with Triton X-100 film has excess PSS, excess Triton X-100 (Tx), Excess PSS interacted with Tx at the surface of PEDOT:PSS film (Figure 6).[30] The PSS polymer is hydrophilic[31] and Tx is surfactant that has both hydrophilic group and hydrophobic group. The SEPT is simple spin coating process with organic solvents (Figure 1). With SEPT, this excess materials can be etched and the microstructure of stretchable PEDOT:PSS can be tuned. Controlling the polarity of solvent that is used in SEPT further can control the amounts of materials that is removed. The solvent with higher polarity shows higher etching ability.

Table 2 is the Hansen solubility parameter (HSP) distance between PSS and various solvents. The Hansen solubility parameter indicates the miscibility of different molecules, and as HSP distance(R) is increased, it means lower miscibility. The hydrophilic PSS shows lower HSP distance value with the polar solvents compare to nonpolar solvents. This miscibility different of PSS is origin of relation

between polarity of solvents and etching ability of SEPT (Table 3.).[32-33] Polar solvent SEPT shows higher etching ability because it can remove excess PSS, whereas nonpolar solvent SEPT cannot remove excess PSS.

This selective etching of PSS with the different polarity of solvent is confirmed with the thickness of stretchable PEDOT:PSS film after SEPT and raman spectroscopy. In figure 7 (a), the remained thickness of stretchable PEDOT:PSS film after SEPT shows a thicker film with lower polarity solvent. As the polarity of the solvent is lower, the thickness is increased. This means that more PSS has remained. This trend is also confirmed in raman spectroscopy (Figure 7 (b)). The peak around 1535 and 1570 cm^{-1} are reported as PSS peaks.[34] After SEPT with polar solvent and nonpolar solvent, the PSS peak is both decreased.[35] However, there are less PSS peak decrease after nonpolar solvent SEPT, meaning more PSS is remained. These experiment results confirm the etching ability depends on solvent polarity.

After SEPT, the large fibril at the surface can be effectively eliminated and microstructure is tuned to a smaller fibril structure by an etching process (Figure 8). This microstructure tuning is confirmed by AFM phase images. Figure 9 (a) is the phase image of stretchable PEDOT:PSS without SEPT, and it shows a large fibril structure. Figure 9 (c), (e) are the phase images of stretchable PEDOT:PSS with SEPT, and each image are processed with a nonpolar solvent and

a polar solvent. In the phase image of PEDOT:PSS the bright regions are conductive PEDOT and the dark regions are insulating PSS. After SEPT, the dark regions are reduced and the fibril structure is also became smaller. We assume that this microstructure tuning is from the gradient fibrous structure of stretchable PEDOT:PSS which has a larger fibril nearby surface and a smaller fibril nearby substrate. After SEPT, a large fibril is etched and a smaller fibril can appear. Figure 9 (b), (d), and (f) is the topology images of each sample. The roughness is increased after SEPT and it shows higher roughness after polar solvent SEPT. This increase in roughness is due to more etched with a polar solvent which coincides with the previous assumption.[36] The redshift (~1430 cm-1) at the Raman shift of both polar solvent and nonpolar solvent SEPT also strengthened the assumption because nonpolar solvent should not supposedly induce phase separation and redshift.

2.4 The Effect of Selective Etching Post Treatment

To study the effect of the SEPT TOF-SIMS depth profile was measured. TOF-SIMS depth profile shows that the microstructure of PEDOT:PSS can affect the amount of PEI that diffuses into PEDOT:PSS film. In TOF-SIMS, SO_3 peaks are from the sulfonated groups in PEDOT:PSS, and NH peaks are from amine groups in PEI. In figure 10(a), PEI only exists at the interface of PEDOT:PSS in the case of PEDOT:PSS without surfactant. The pristine PEDOT:PSS does not show a large fibril structure like stretchable PEDOT:PSS (Figure 4 (a)). Therefore, the PEI diffusion can be prevented. However, the severe diffusion of PEI is occurred at stretchable PEDOT:PSS with a fibril structure (figure 10(b)). This diffusion of PEI can be prevented by microstructure tuning after SEPT (figure 10(c)). With TOF-SIMS depth profile, the successful PEI diffusion prevention with microstructure tuning of stretchable PEDOT:PSS with SEPT was confirmed.

The I-V curve change is also tested to check the relationship between PEDOT:PSS microstructure and PEI diffusion. After the PEI solution is coated onto PEDOT:PSS film, a certain time was waited before spin coating to give enough time for PEI diffuse into PEDOT:PSS film (Figure 11 (a)). The slope of the I-V curve means the 1/R. By measuring resistance change of PEDOT:PSS film, we could measure the preventing effect of SEPT. The resistance of stretchable PEDOT:PSS without SEPT film increased around 128% after 1 minute of waiting,

however with SEPT, there is no I-V curve change. After 10 minutes of waiting, the change of slope is more significant. Without SEPT film, the R increased by around 471% but with SEPT film shows less decrease which is around 140% (Figure 11 (b),(c)).

By suppressing the PEI diffusion into stretchable PEDOT:PSS film, severe de-doping of PEDOT can be prevented. The high work function stretchable PEDOT:PSS without PEI coated shows sheet resistance around 261 ohm/sq. After PEI coating without SEPT, this sheet resistance increases up to 537 ohm/sq which is more than double compared to the pristine value. With the SEPT, the significant increase in sheet resistance can be prevented and the low sheet resistance value around 237 ohm/sq can be achieved while the work function is also effectively lowered to 3.84 eV from 4.72 eV (Figure 12 (a), (b)). To exclude the thickness dependency of PEDOT:PSS film electrode, the resistivity of PEI coating without SEPT and PEI coating with polar solvent SEPT were also measured because they have a similar thickness (~87 nm). As expected, the resistivity with SEPT film was smaller than without SEPT film after PEI coating (Table 4). This low WF stretchable PEDOT:PSS has high transparency around 96.7 % at a wavelength of 550 nm and we achieve the Figure of Merit (FoM) value around 47 which is enough for practical use (Figure 12 (c)).[37]

2.5 The Stretchability after Selective Etching Post Treatment

During SEPT, PSS at the surface of PEDOT:PSS is removed. Since PSS is soft domain among PEDOT:PSS, the removal of soft PSS domain cause the sacrifice of stretchability. To minimize the stretchability sacrifice, it is important to remain PSS after the SEPT. Therefore, solvent selection for SEPT is highly important. The amount of remained PSS can be controlled by solvent polarity control, and stretchability sacrifice can be minimized.[18]

To determine the stretchability of PEDOT:PSS film with different kinds of solvent, crack onset strain is measured (Figure 13 (a)). To measure stretchability, the stretchable PEDOT:PSS film is coated onto soft substrate (SEBS), then additional thin SEBS layer is encapsulated over PEDOT:PSS film to give additional stretchability by compression.[4] As polarity of solvent for SEPT increased, the crack onset strain is decreased. After SEPT with 2-methoxyethanol which has high polarity, the cracks on PEDOT:PSS film occurs only before the 30 %. However, toluene which is nonpolar solvent showed the highest crack onset strain that reaches around 50 %. The stretchable PEDOT:PSS with nonpolar solvent SEPT, also shows lower resistance change at stretching test. With the static stretching test and cyclic stretching test, the SEPT with toluene shows less strain sensitivity. The SEPT with toluene film only had a normalized resistance change

(R/R_0) of 1.77 at strain =50%, while resistance change reached over 3 in the case of polar solvent SEPT film. (Figure 13 (b)) This superior stretchability trend was also observed in the cyclic stretching test at strain = 30% for 500 cycles (Figure (13 (c), (d), (e)). From these analysis, toluene which is nonpolar solvent was used as solvent of SEPT.

The formation of PEI film is also a solution process so the selection of PEI solvent is also important. The PEI is a hydrophilic polymer, therefore polar solvent should be used to disperse PEI. From the stretchability test, IPA shows less strain sensitivity compare to 2-methoxyethanol which is widely used as a PEI solvent.

2.6 Device characteristics

ISOLED is fabricated based with stretchable PEDOT:PSS as anode and cathode. The device structure and band diagram are shown in Figure 14. Widely used vacuum deposited cathode cannot be used in intrinsically stretchable display due to its poor mechanical property.[38] Direct spin coating of PEDOT:PSS onto emitting layer (EML) can cause EML degradation which leads the poor luminance property and lifetime.[5, 39] Lamination process was chosen to fabricate top electrode because this process can successfully stack stretchable top electrode while avoiding solvent attack.[40-41]

The lamination process uses only physical adhesion, therefore heat and pressure must be precisely controlled. If the heat or pressure is not sufficient, then two different interfaces cannot be laminated. However, emitting layer or electrode can degrade if the heat or pressure is overly treated. Our group previously reported the pressure-controlled lamination process. From our knowledge, 100 °C and 50 kPa can give sufficient power to laminate two different interfaces while protecting emitting layer from degradation. We measure I-V curve to evaluate the stability of PEDOT:PSS electrode during lamination condition. In the figure 15, there are no I-V curve change under 100 °C and 50 kPa for 20 mins. It means that there are no PEDOT:PSS degradation and no further PEI diffusion during lamination process.

The light-emitting characteristics were measured to evaluate effect of

SEPT (Figure 16). At the low voltage, there are high leakage current, but this problem was from the pixel defining issue. At the high voltage, stretchable light emitting with SEPT shows higher current density and luminance. This experimental result implies that de-doping of PEDOT with SEPT is successfully prevented, and the conductivity of electrode was significantly improved as expected. Based on low WF stretchable PEDOT:PSS electrode, the size of 6 mm x 3 mm stretchable LED was demonstrated with uniform light-emitting in whole pixel (Figure 17).

2.7 Experimental

Materials

PEDOT:PSS (Clevious™ P PH 1000, Clevious™ P AI 4083) were purchased from Heraeus. Triton X™ -100, dimethyl sulfoxide (DMSO, 99.8%, anhydrous), polyethyleneimine (PEI, branched M_w ~ 270,000), Super Yellow (PDY-132, M_w ~ 1,300,000), cyclohexanone(99.8%, anhydrous), toluene (99.8%, anhydrous), and 2-methoxyethanol (99.8% anydrous) were purchased from Sigma-Aldrich.

Fabrication of stretchable PEDOT:PSS electrode.

In PEDOT:PSS (Clevious P PH 1000) solution, 5 wt% of DMSO and 5 wt% of Triton X was added. The solution was mixed in a roller for less than 1 hour. This PEDOT:PSS solution is then spin-coated at the stretchable substrate. The stretchable substrate is composite structure of Styrene Ethylene/Butylene Styrene (SEBS) and polydimethylsiloxane (PDMS). The stretchable PEDOT:PSS solutions were spin-coated with roatating speed of 2000 rpm, 60 s. Then the films were annealed on a hot plate at 100°C for 10 min. For cathode, PEI is overcoated onto stretchable PEDOT:PSS film with rotating speed of 5000rpm, 60s and annealed at 100°C for 10 min.

Fabrication of intrinsically stretchable light-emitting diode.

PEDOT:PSS (Clevious^{TM} P VP AI 4083) is used as hole injection layer (HIL). To achieve stretchable HIL, 5 wt% of Triton X-100 was added into AI 4083 solution which was diluted by IPA at a 1:1 weight ratio. The Super Yellow (PDY-132) is used as stretchable emitting layer (EML). In the co-solvent (Cyclohexanone : toluene at a volume ration of 4: 1), 6 mg/mL of the Super Yellow and 1.2 mg/mL of the Triton X-100 was added. On the PEDOT:PSS anode which was patterned by PDMS stamping, stretchable EML was spin coated at 3000rpm, 60s and annealed at 90 ℃ for 5 min in an N_2- filled glove box. The lamination process was performed to contact EML and low WF stretchable PEDOT:PSS cathode.

Characterizations method.

To measure sheet resistance of PEDOT:PSS film, 4-point probe was used. The UV absorbance and optical transmittance were measured by using UV absorption spectroscopy (Lambda 465, PerkinElmer). The work function of stretchable PEDOT:PSS film was measured using Kelvin probe (SKP-5050, KP Technology Ltd). The Raman spectroscopy was performed by a LabRAM HR Evolution (HORIBA), and the wavelength of laser was 532 nm. AFM images were obtained using a NX-10 at the Research Institute of Advanced Materials. TOF SIMS depth profile obtained with TOF SIMS-5 (ION TOF, Germany). I-V curve to

measure PEI diffusion test and electrode stability test during lamination process, the Keithley 2400 source meter was used. During static stretching test, the strain was applied with a stretching rate 10mm/min. To measure cyclic stretching test, the strain was applied up to 30% and released back to 0%. This cycles were conducted for 500 times to measure cyclic stretching test. Lastly, the current-voltage-luminance characteristics of stretchable displays were measured with using source-measurement unit (Keithley 236), a spectroradiometer (CS-2000, Konia Minolta).

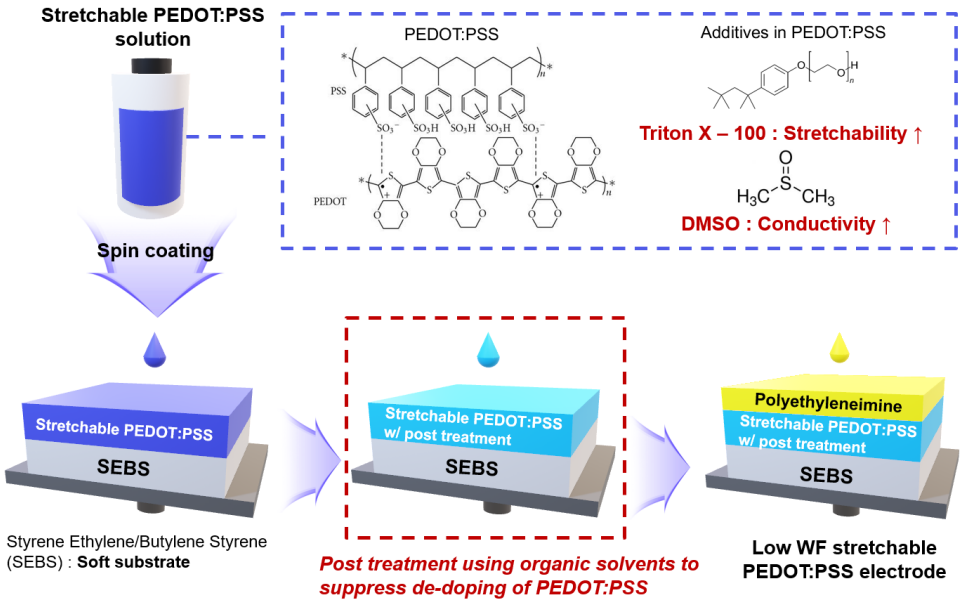

Figure 1. The fabrication process of low work function stretchable PEDOT:PSS

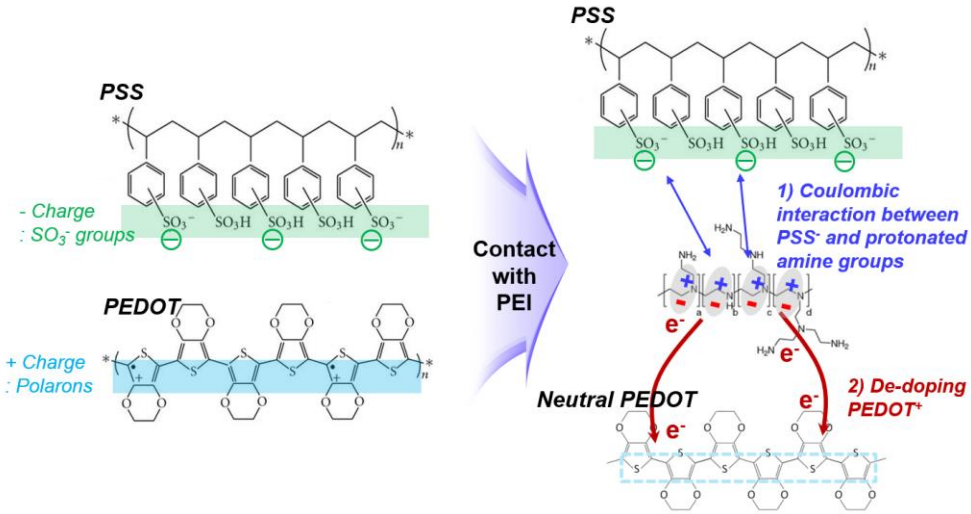

Figure 2. The de-doping mechanism of PEDOT:PSS with PEI

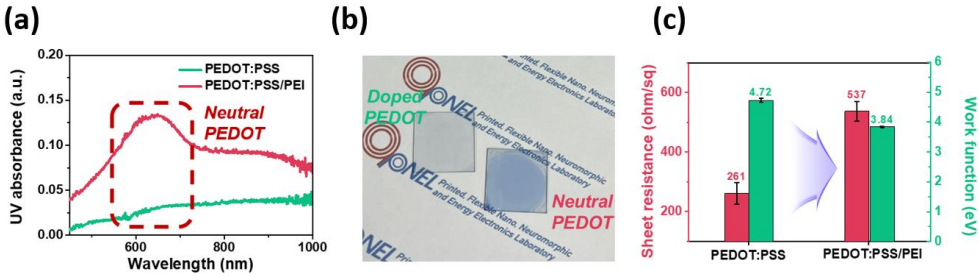

Figure 3. (a) UV absorbance of stretchable PEDOT:PSS before PEI coating (doped PEDOT) and after PEI coating (neutral PEDOT). (b) Optical image of doped PEDOT and neutral PEDOT. (c) Sheet resistance and work function of stretchable PEDOT:PSS before PEI coating and after PEI coating.

Sheet resistance (R_s) of PEDOT:PSS film			
	w/o PEI (R_0)	**w/ PEI (R)**	***R/R_0***
PEDOT:PSS w/o additives	220	197	**0.89**
Stretchable PEDOT:PSS	261	537	**2.06**

Table 1. Sheet resistance of PEDOT:PSS without additives and stretchable PEDOT:PSS before spin coating PEI and after spin coating PEI.

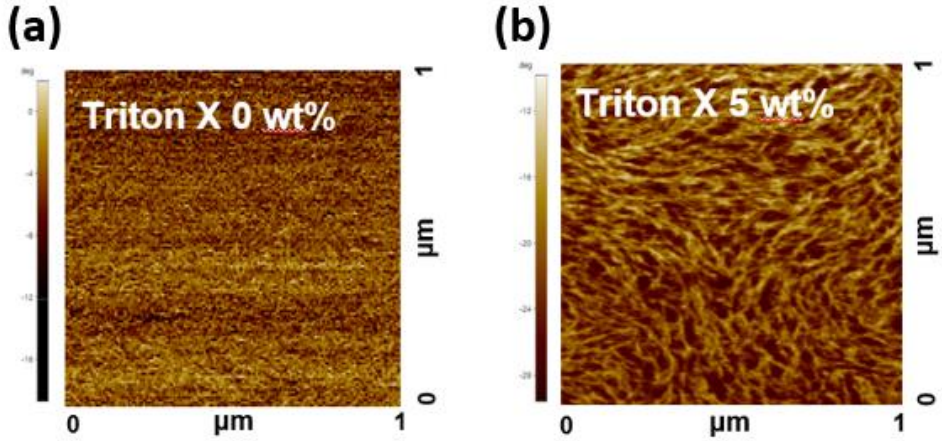

Figure 4. (b) AFM phase image of PEODT:PSS without additives, (c) AFM phase images of stretchable PEDOT:PSS with Triton X -100 5 wt%.

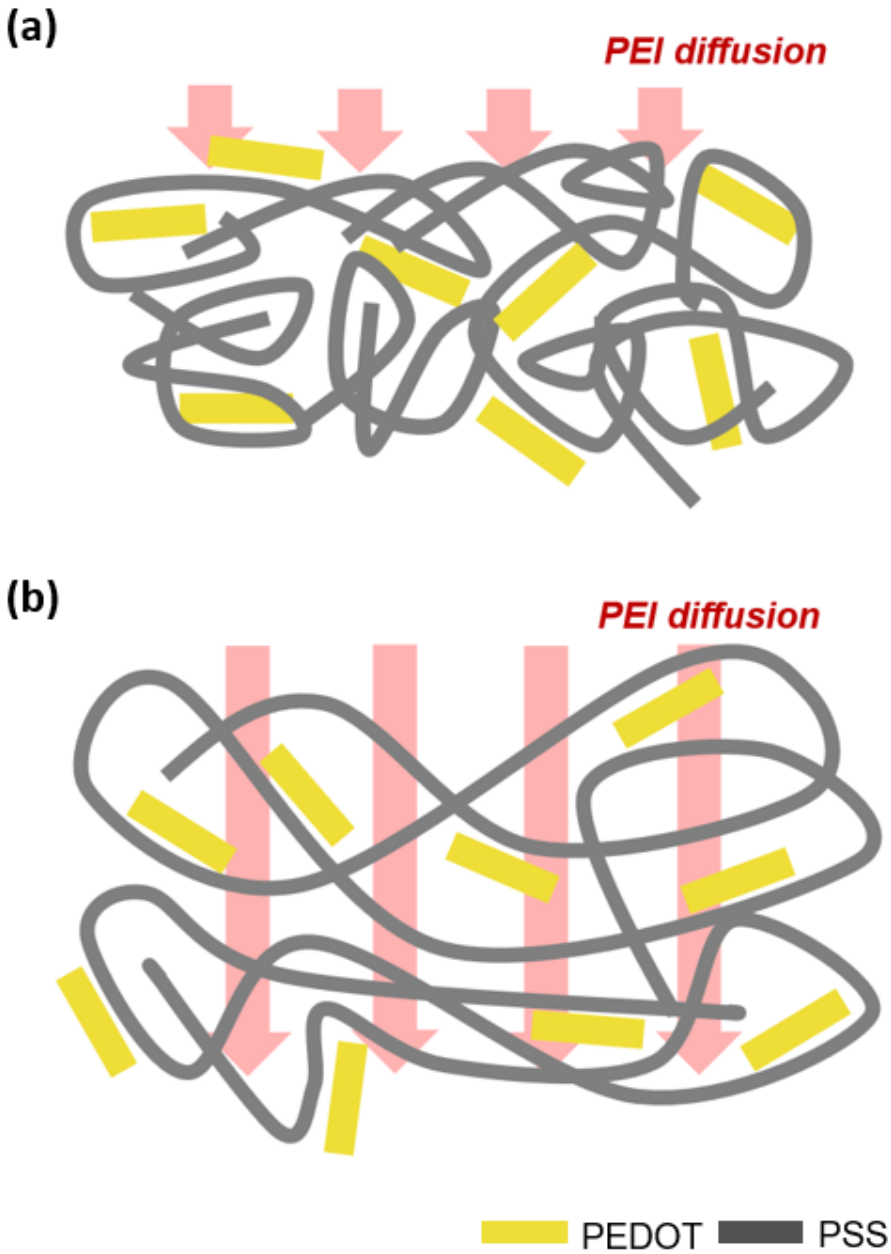

Figure 5. (a) Schematic illustration of PEDOT:PSS w/o additives microstructure.

(b) Schematic illustration of stretchable PEDOT:PSS microstructure

Figure 6. Schematic illustration of the surface of Triton X treated PEDOT:PSS.

HSP distance of PSS with selective etching post treatment solvents				
	δ_d [Mpa]$^{1/2}$	δ_p [Mpa]$^{1/2}$	δ_h [Mpa]$^{1/2}$	HSP distance (R)
PSS	**20.5**	**12.4**	**15.9**	-
1-Butanol	16	5.7	15.8	11.22052
IPA	15.8	6.1	16.4	11.32696
Hexane	14.9	14.9	0	16.45053
Toluene	18	1.4	2	18.41765

Table 2. Hansen solubility parameter distance of PSS and solvents with different polarity.

Washed away ?	Polar solvent	Nonpolar solvent
PSS	O	X
Triton X	O	O
Triton X w/ PSS	O	O

Table 3. Selective etching of surface existed polymers and molecules by solvent polarity control.

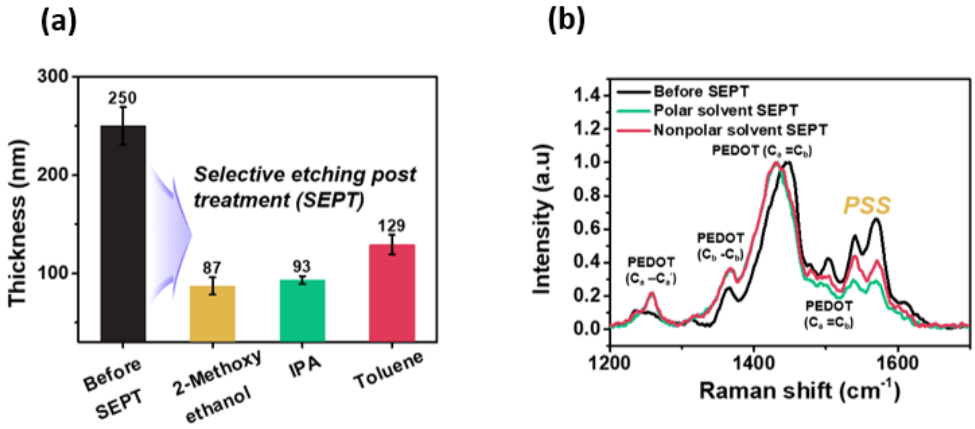

Figure 7. (a) Thickness change after SEPT with different polarity of solvent. (b) Raman spectroscopy of stretchable PEDOT:PSS without SEPT, polar solvent and nonpolar solvent.

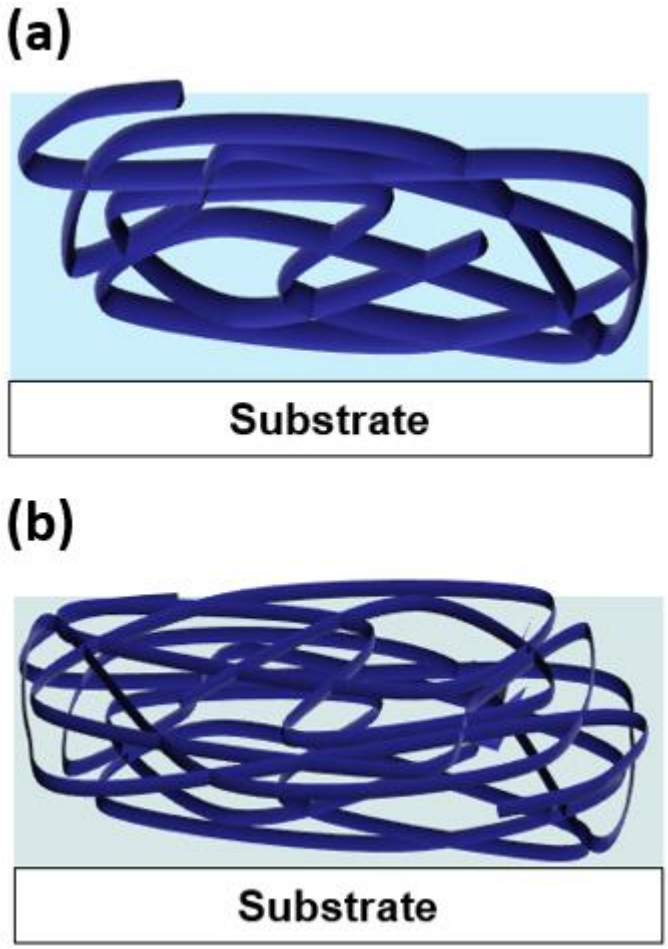

Figure 8. Schematic illustration of the mechanism of microstructure tuning with selective etching post treatment (SEPT). (a) Before SEPT (b) After SEPT

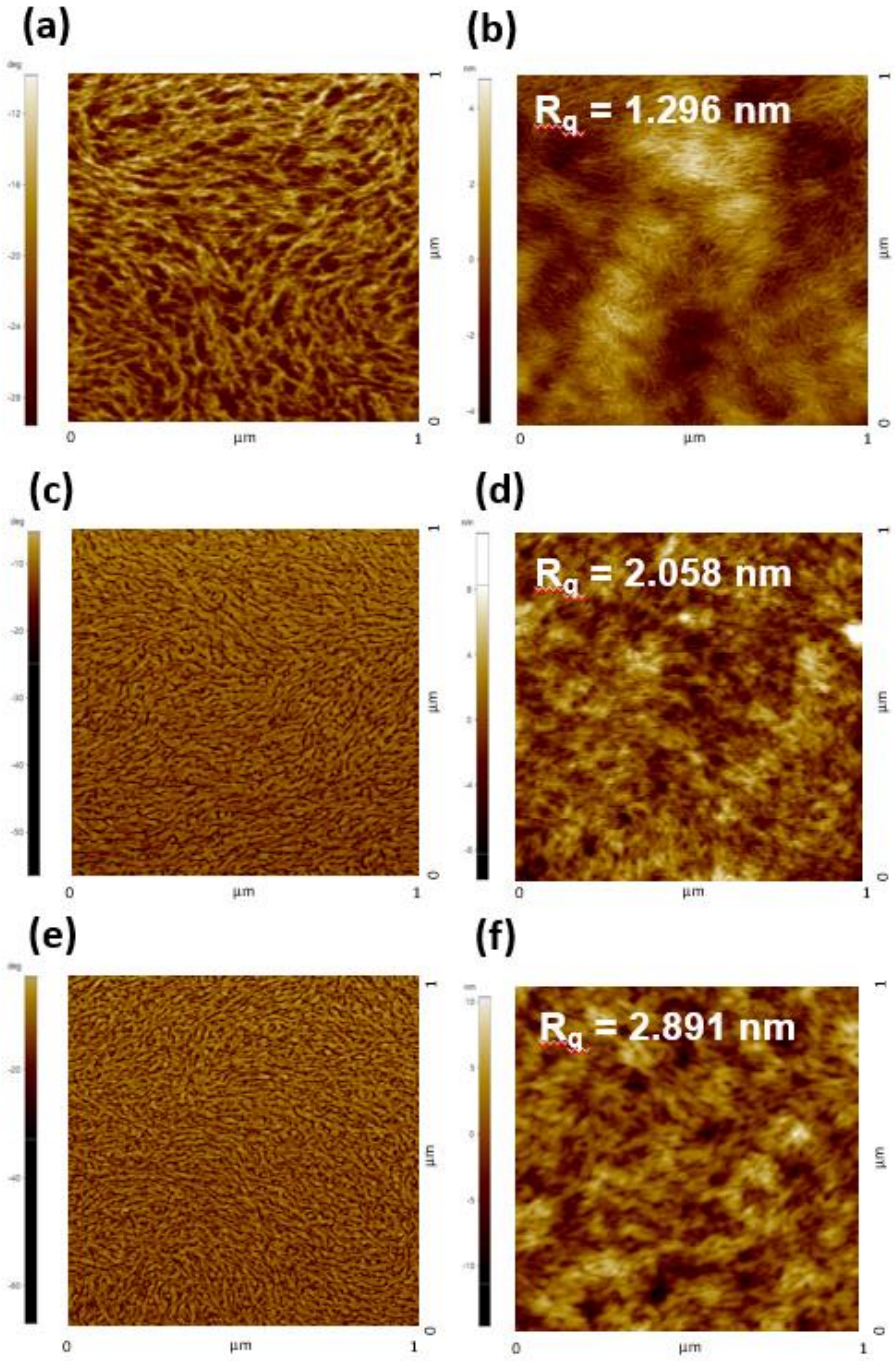

Figure 9. AFM phase images of: (a) without SEPT, (b) polar solvent SEPT (c) nonpolar solvent SEPT. AFM topology images of: (a) without SEPT, (b) polar solvent SEPT (c) nonpolar solvent SEPT

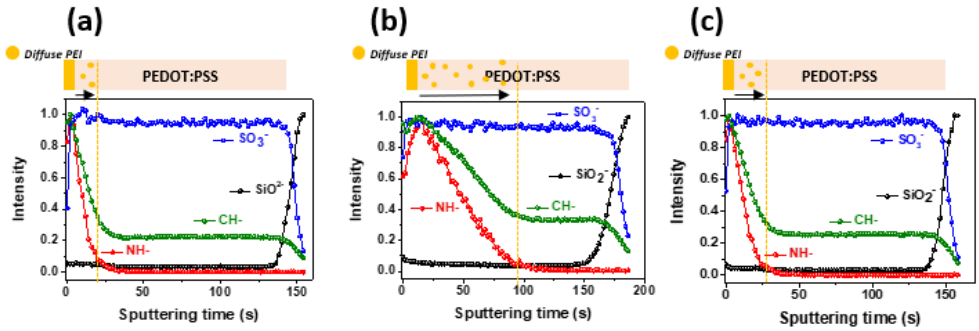

Figure 10. TOF SIMS depth profile of PEI spin coated on the pristine PEDOT:PSS, stretchable PEDOT:PSS without SEPT, and stretchable PEDOT:PSS with SEPT.

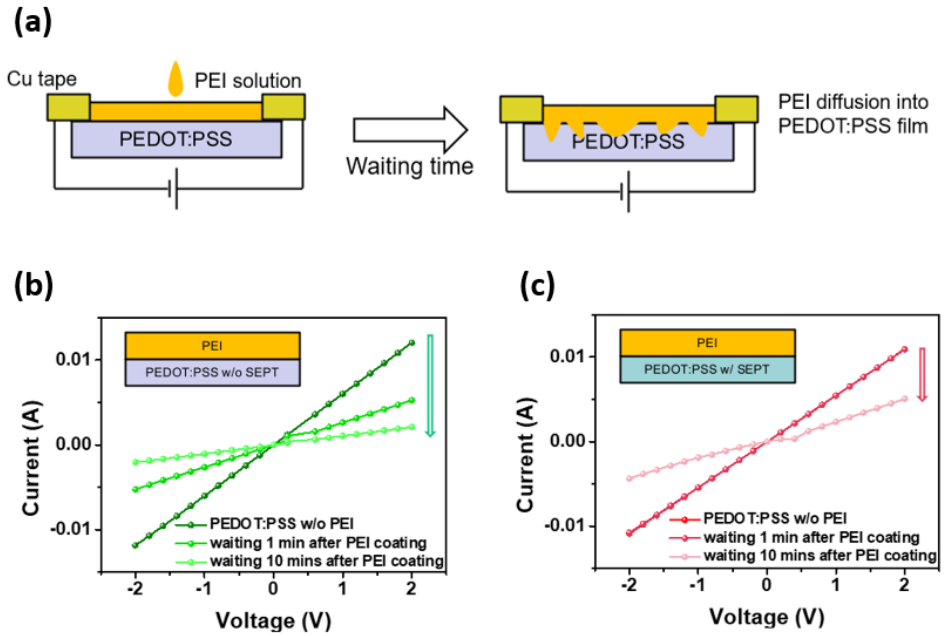

Figure 11. (a) Schematic illustration of experiment process to measure PEI diffusion into stretchable PEDOT:PSS film. (b),(c) I-V curve with waiting time after PEI coating on the stretchable PEDOT:PSS film without SEPT and with SEPT.

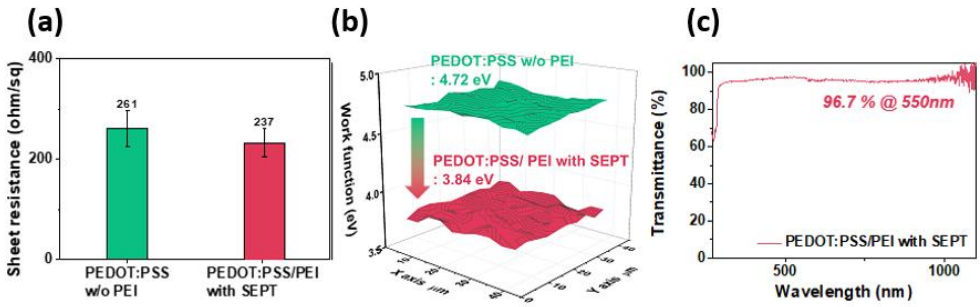

Figure 12. (a) Sheet resistance of high WF stetchable PEDOT:PSS without PEI, PEI coated low WF stretchable PEDOT:PSS without SEPT and with SEPT. (b) Kelvin probe mapping of WF of stretchable PEDOT:PSS before and after PEI coating. (c) Transmittance of low WF stretchable PEDOT:PSS with SEPT.

Resistivity (Sheet resistance x thickness) (Ωm)	
PEI coating without SEPT	PEI coating with SEPT (2-Methoxyethanol)
$2.06 * 10^{-5}$	$4.67 * 10^{-5}$

Table 4. The resistivity value of PEI coating without SEPT and PEI coating with polar solvent SEPT (2-Methoxyethanol)

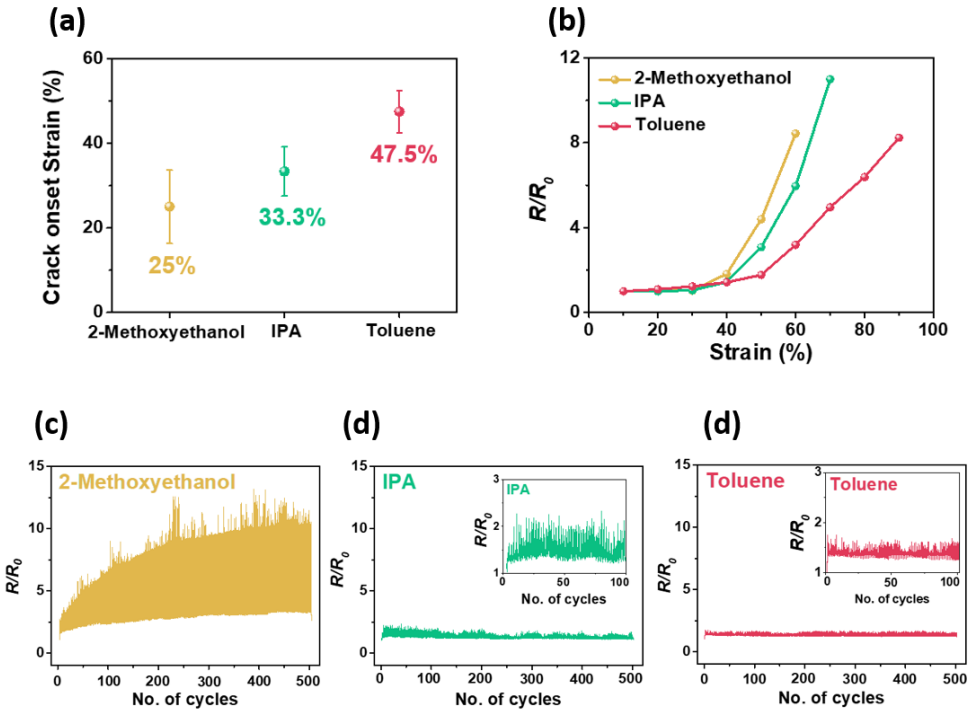

Figure 13. (a) Crack onset strain of stretchable PEDOT:PSS with SEPT by 2-methoxyethanol, IPA and toluene. (b) Static stretching tests of stretchable PEDOT:PSS with SEPT by 2-methoxyethanol, IPA and toluene. (c),(d),(e) Cyclic stretching tests of stretchable PEDOT:PSS with SEPT by 2-methoxyethanol, IPA and toluene

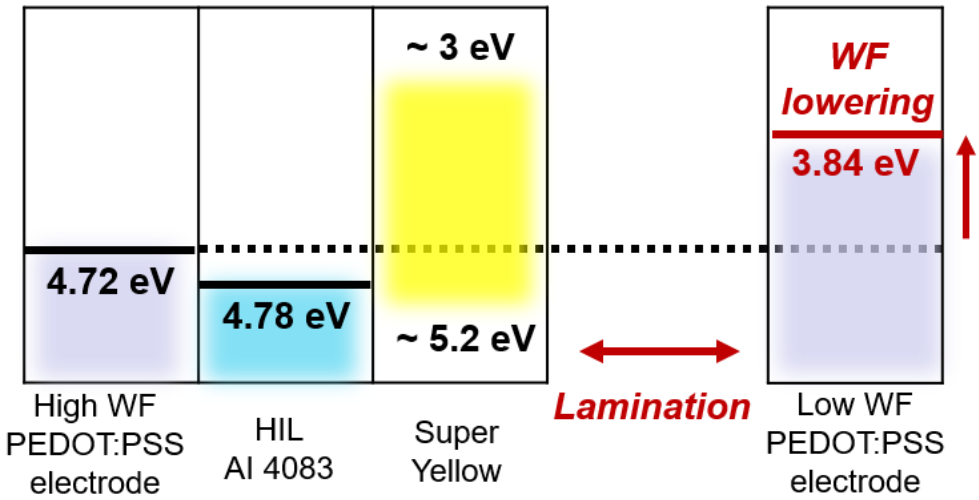

Figure 14. Energy band diagram of stretchable LED.

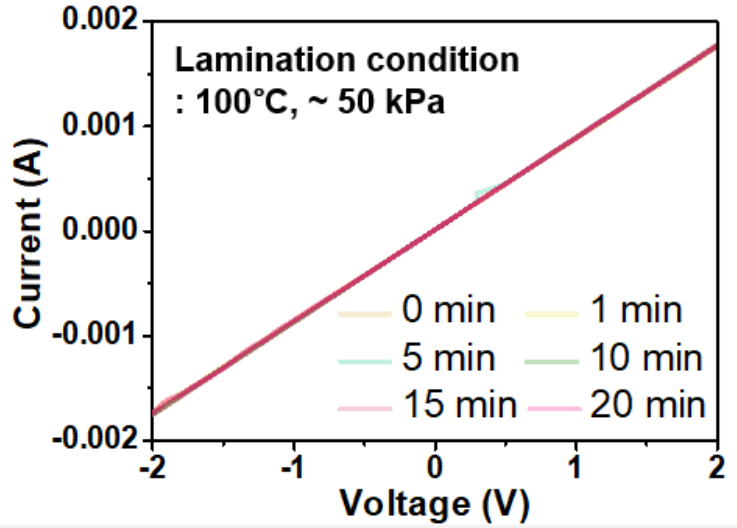

Figure 15. Stretchable PEDOT:PSS electrode stability test by I-V curve with increasing time from 0 to 20 mins in lamination condition (100°C and 50 kPa).

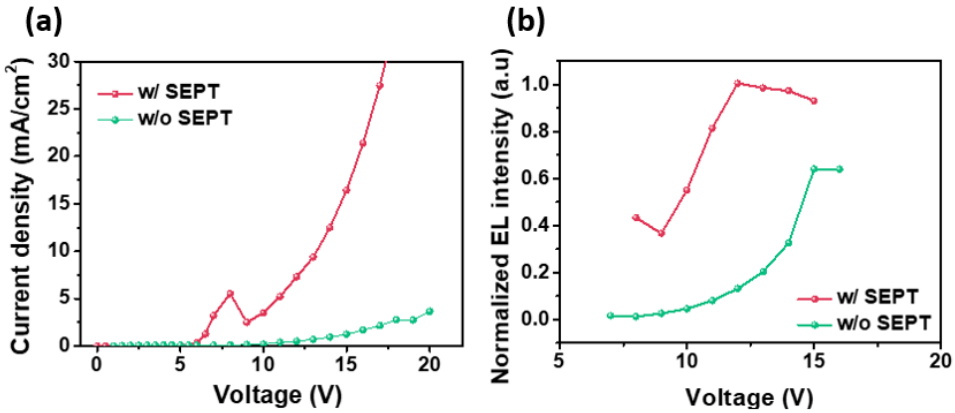

Figure 16. Current density-voltage-luminance (J-V-L) characteristics of intrinsically stretchable LED without SEPT and with SEPT.

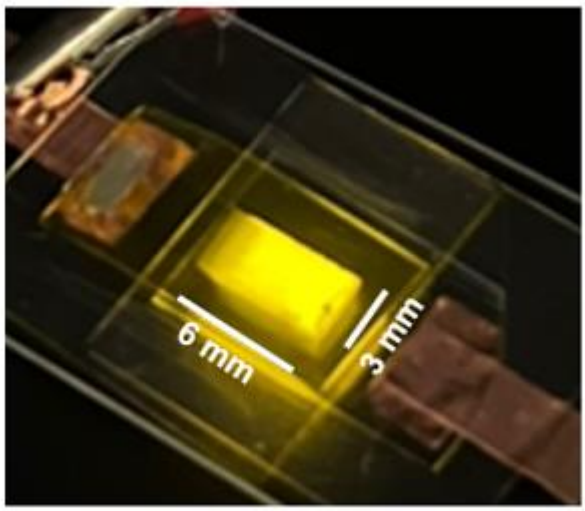

Figure 17. Uniform pixel emission in intrinsically stretchable LED.

Chapter 3. Conclusion

We have demonstrated a stretchable PEDOT:PSS electrode for electron injection in intrinsically stretchable light-emitting diodes. By introducing selective etching post treatment (SEPT), the microstructure of stretchable PEDOT:PSS has been successfully tuned from large fibril to smaller fibril. The underlying mechanism of SEPT is the different miscibility between hydrophilic PSS and the polarity of the solvent that is used in SEPT. Using this method, we could prevent the PEI diffusion into PEDOT:PSS, and the amount of PEDOT that can be de-doped with PEI is also suppressed to PEDOT only at the surface. Also, by selecting a nonpolar solvent SEPT, the remained PSS after SEPT were increased compared to polar solvent SEPT. Using this tactic, the microstructure can be tuned while minimizing the stretchability sacrifice of PEDOT:PSS film. The work function of stretchable PEDOT:PSS was lowered from 4.78 eV to 3.84 eV without any electrical conductivity decrease. This low WF stretchable PEDOT:PSS film shows superior stretchability with stable resistance change under the cyclic stretching test at strain 30%. Finally, intrinsically stretchable light-emitting diodes were demonstrated with stretchable PEDOT:PSS anode and cathode. The lamination process was performed to stack the top electrode, and we achieved uniform light-emitting in the 6 mm x 3 mm size of the pixel.

Bibliography

[1] Z. Zhang, W. Wang, Y. Jiang, Y.-X. Wang, Y. Wu, J.-C. Lai, S. Niu, C. Xu, C.-C. Shih, C. Wang, H. Yan, L. Galuska, N. Prine, H.-C. Wu, D. Zhong, G. Chen, N. Matsuhisa, Y. Zheng, Z. Yu, Y. Wang, R. Dauskardt, X. Gu, J. B. H. Tok, Z. Bao, *Nature* **2022**, *603*, 624-630.

[2] S. G. R. Bade, X. Shan, P. T. Hoang, J. Li, T. Geske, L. Cai, Q. Pei, C. Wang, Z. Yu, *Advanced Materials* **2017**, *29*, 1607053.

[3] J. Liang, L. Li, X. Niu, Z. Yu, Q. Pei, *Nature Photonics* **2013**, *7*, 817-824.

[4] H. Zhou, S. J. Han, A. K. Harit, D. H. Kim, D. Y. Kim, Y. S. Choi, H. Kwon, K.-N. Kim, G.-T. Go, H. J. Yun, B. H. Hong, M. C. Suh, S. Y. Ryu, H. Y. Woo, T.-W. Lee, *Advanced Materials* **2022**, *34*, 2203040.

[5] J.-H. Kim, J.-W. Park, *Science Advances* **2021**, *7*, eabd9715.

[6] J. A. Rogers, T. Someya, Y. Huang, *Science* **2010**, *327*, 1603-1607.

[7] R.-H. Kim, D.-H. Kim, J. Xiao, B. H. Kim, S.-I. Park, B. Panilaitis, R. Ghaffari, J. Yao, M. Li, Z. Liu, V. Malyarchuk, D. G. Kim, A.-P. Le, R. G. Nuzzo, D. L. Kaplan, F. G. Omenetto, Y. Huang, Z. Kang, J. A. Rogers, *Nature Materials* **2010**, *9*, 929-937.

[8] M. S. Lim, M. Nam, S. Choi, Y. Jeon, Y. H. Son, S.-M. Lee, K. C. Choi, *Nano Letters* **2020**, *20*, 1526-1535.

[9] Z. Yu, X. Niu, Z. Liu, Q. Pei, *Advanced Materials* **2011**, *23*, 3989-3994.

[10] J. Liu, J. Wang, Z. Zhang, F. Molina-Lopez, G.-J. N. Wang, B. C. Schroeder, X. Yan, Y. Zeng, O. Zhao, H. Tran, T. Lei, Y. Lu, Y.-X. Wang, J. B. H. Tok, R. Dauskardt, J. W. Chung, Y. Yun, Z. Bao, *Nature*

Communications **2020**, *11*, 3362.

[11] J. Liang, L. Li, K. Tong, Z. Ren, W. Hu, X. Niu, Y. Chen, Q. Pei, *ACS Nano* **2014**, *8*, 1590-1600.

[12] Y. Wang, C. Zhu, R. Pfattner, H. Yan, L. Jin, S. Chen, F. Molina-Lopez, F. Lissel, J. Liu, N. I. Rabiah, Z. Chen, J. W. Chung, C. Linder, M. F. Toney, B. Murmann, Z. Bao, *Science Advances* **2017**, *3*, e1602076.

[13] I. Lee, G. W. Kim, M. Yang, T.-S. Kim, *ACS Applied Materials & Interfaces* **2016**, *8*, 302-310.

[14] L.-W. Lo, J. Zhao, H. Wan, Y. Wang, S. Chakrabartty, C. Wang, *ACS Applied Materials & Interfaces* **2021**, *13*, 21693-21702.

[15] Y. H. Kim, C. Sachse, M. L. Machala, C. May, L. Müller-Meskamp, K. Leo, *Advanced Functional Materials* **2011**, *21*, 1076-1081.

[16] J. Y. Oh, S. Kim, H.-K. Baik, U. Jeong, *Advanced Materials* **2016**, *28*, 4455-4461.

[17] R. Luo, H. Li, B. Du, S. Zhou, Y. Zhu, *Organic Electronics* **2020**, *76*, 105451.

[18] S. Savagatrup, E. Chan, S. M. Renteria-Garcia, A. D. Printz, A. V. Zaretski, T. F. O'Connor, D. Rodriquez, E. Valle, D. J. Lipomi, *Advanced Functional Materials* **2015**, *25*, 427-436.

[19] E. Dauzon, Y. Lin, H. Faber, E. Yengel, X. Sallenave, C. Plesse, F. Goubard, A. Amassian, T. D. Anthopoulos, *Advanced Functional Materials* **2020**, *30*, 2001251.

[20] M. Y. Teo, N. Kim, S. Kee, B. S. Kim, G. Kim, S. Hong, S. Jung, K. Lee, *ACS Appl Mater Interfaces* **2017**, *9*, 819-826.

[21] S. Kee, H. Kim, S. H. K. Paleti, A. El Labban, M. Neophytou, A.-H.

Emwas, H. N. Alshareef, D. Baran, *Chemistry of Materials* **2019**, *31*, 3519-3526.

[22] S.-H. Jeong, H. Kim, M.-H. Park, Y. Lee, N. Li, H.-K. Seo, T.-H. Han, S. Ahn, J.-M. Heo, K. S. Kim, T.-W. Lee, *Nano Energy* **2019**, *60*, 324-331.

[23] Y. Zhou, C. Fuentes-Hernandez, J. Shim, J. Meyer, A. J. Giordano, H. Li, P. Winget, T. Papadopoulos, H. Cheun, J. Kim, M. Fenoll, A. Dindar, W. Haske, E. Najafabadi, T. M. Khan, H. Sojoudi, S. Barlow, S. Graham, J. L. Brédas, S. R. Marder, A. Kahn, B. Kippelen, *Science* **2012**, *336*, 327-332.

[24] S. Fabiano, S. Braun, X. Liu, E. Weverberghs, P. Gerbaux, M. Fahlman, M. Berggren, X. Crispin, *Advanced Materials* **2014**, *26*, 6000-6006.

[25] T. P. A. van der Pol, S. T. Keene, B. W. H. Saes, S. C. J. Meskers, A. Salleo, Y. van de Burgt, R. A. J. Janssen, *The Journal of Physical Chemistry C* **2019**, *123*, 24328-24337.

[26] S. T. Keene, T. P. A. van der Pol, D. Zakhidov, C. H. L. Weijtens, R. A. J. Janssen, A. Salleo, Y. van de Burgt, *Advanced Materials* **2020**, *32*, 2000270.

[27] W. Cai, T. Österberg, M. J. Jafari, C. Musumeci, C. Wang, G. Zuo, X. Yin, X. Luo, J. Johansson, M. Kemerink, L. Ouyang, T. Ederth, O. Inganäs, *Journal of Materials Chemistry C* **2020**, *8*, 328-336.

[28] Y. Xuan, M. Sandberg, M. Berggren, X. Crispin, *Organic Electronics* **2012**, *13*, 632-637.

[29] S. Bontapalle, A. Opitz, R. Schlesinger, S. R. Marder, S. Varughese, N. Koch, *Advanced Materials Interfaces* **2020**, *7*, 2000291.

[30] S.-S. Yoon, D.-Y. Khang, *The Journal of Physical Chemistry C* **2016**, *120*, 29525-29532.

[31] J. J. Lee, S. Gandla, B. Lim, S. Kang, S. Kim, S. Lee, S. Kim, *NPG Asia Materials* **2020**, *12*, 65.

[32] W. H. Ferrell, D. I. Kushner, M. A. Hickner, *Journal of Polymer Science Part B: Polymer Physics* **2017**, *55*, 1365-1372.

[33] M. Belmares, M. Blanco, W. A. Goddard III, R. B. Ross, G. Caldwell, S.-H. Chou, J. Pham, P. M. Olofson, C. Thomas, *Journal of Computational Chemistry* **2004**, *25*, 1814-1826.

[34] T. A. Yemata, Y. Zheng, A. K. K. Kyaw, X. Wang, J. Song, W. S. Chin, J. Xu, *RSC Advances* **2020**, *10*, 1786-1792.

[35] Y. Kim, W. Cho, Y. Kim, H. Cho, J. H. Kim, *Journal of Materials Chemistry C* **2018**, *6*, 8906-8913.

[36] Y.-S. Hsiao, W.-T. Whang, C.-P. Chen, Y.-C. Chen, *Journal of Materials Chemistry* **2008**, *18*, 5948-5955.

[37] M. Vosgueritchian, D. J. Lipomi, Z. Bao, *Advanced Functional Materials* **2012**, *22*, 421-428.

[38] S. P. Lacour, D. Chan, S. Wagner, T. Li, Z. Suo, *Applied Physics Letters* **2006**, *88*, 204103.

[39] S. Ahn, W. Jang, S. Park, D. H. Wang, *ACS Applied Materials & Interfaces* **2017**, *9*, 15623-15630.

[40] D. Gupta, M. M. Wienk, R. A. J. Janssen, *Advanced Energy Materials* **2013**, *3*, 782-787.

[41] T.-F. Guo, S. Pyo, S.-C. Chang, Y. Yang, *Advanced Functional Materials* **2001**, *11*, 339-343.

Abstract

PEDOT:PSS는 높은 전도도와 우수한 안전성 특성을 가지며 이에 따라서 기존에 사용되고 있는 ITO 전극을 대체할 수 있는 신축성 전극의 후보군으로 연구되고 있다. 하지만 PEDOT:PSS의 높은 전기적 특성과 신축성을 유지한 상태로 일함수를 조절하는 것은 매우 도전적이다. 본 연구에서는, PEDOT:PSS의 표면처리를 통해 전도도와 신축성을 유지하면서 일함수를 조절할 수 있다. Polyethyleneimine (PEI)를 PEDOT:PSS 위에 코팅 시, 계면 사이에 원치 않은 화학적 반응이 일어난다. 이는 디도핑 반응이라 하며, 전도도가 급감하는 현상이 나타난다. 큰 피브릴 구조를 갖는 신축성 PEDOT:PSS에서는 PEI가 PEDOT:PSS film 내부로 더 깊게 확산 될 수 있으며, 이에 따라서 디도핑 현상이 더 강하게 나타난다. 본 연구에서는 미세구조를 조절함으로써, PEI의 확산을 방지했으며 디도핑 반응이 표면에서만 나타날 수 있도록 억제하는데 성공했다. 결과적으로 3.84 eV라는 낮은 일함수를 갖는 PEDOT:PSS 전극을 개발할 수 있었고 이를 적용한 고유 신축성 유기 발광 다이오드를 제작했다. 해당 연구를 통해서 신축성 전극과 신축성 LED 개발에 사용될 수 있는 다기능성을 확보한 PEDOT:PSS 전극을 개발했다.